LETTER

Torsional moduli of transition metal dichalcogenide nanotubes from first principles

Arpit Bhardwaj, Abhiraj Sharma and Phanish Suryanarayana*

College of Engineering, Georgia Institute of Technology, Atlanta, GA 30332, USA.

E-mail: phanish.suryanarayana@ce.gatech.edu

Abstract. We calculate the torsional moduli of single-walled transition metal dichalcogenide (TMD) nanotubes using *ab initio* density functional theory (DFT). Specifically, considering forty-five select TMD nanotubes, we perform symmetry-adapted DFT calculations to calculate the torsional moduli for the armchair and zigzag variants of these materials in the low-twist regime and at practically relevant diameters. We find that the torsional moduli follow the trend: $MS_2 > MSe_2 > MTe_2$. In addition, the moduli display a power law dependence on diameter, with the scaling generally close to cubic, as predicted by the isotropic elastic continuum model. In particular, the shear moduli so computed are in good agreement with those predicted by the isotropic relation in terms of the Young's modulus and Poisson's ratio, both of which are also calculated using symmetry-adapted DFT. Finally, we develop a linear regression model for the torsional moduli of TMD nanotubes based on the nature/characteristics of the metal-chalcogen bond, and show that it is capable of making reasonably accurate predictions.

Keywords: Torsional modulus, Transition Metal Dichalcogenides, Nanotubes, Density Functional Theory, Shear modulus, Young's modulus, Poisson's ratio

Supplementary material for this article is available online.

1. Introduction

The synthesis of carbon nanotubes around three decades ago [1] has revolutionalized the fields of nanoscience and nanotechnology. Even in the specific instance of nanotubes — quasi one-dimensional hollow cylindrical structures with diameters in the nanometer range — nearly two dozen nanotubes have now been synthesized [2, 3, 4], with the potential for thousands more given the large number of stable two-dimensional materials that have been predicted from first principles calculations [5, 6, 7]. Nanotubes have been the subject of intensive research, inspired by the novel and enhanced mechanical, electronic, optical, and thermal properties relative to their bulk counterparts [2, 3, 4].

Nanotubes can be categorized based on the classification adopted for the corresponding two-dimensional materials from which they can be thought to be

constructed. Among the different groups, the transition metal dichalcogenide (TMD) group — materials of the form MX_2, where M and X represent a transition metal and chalcogen, respectively — is currently the most diverse, particularly given that they contain the largest number of distinct nanotubes synthesized to date [2, 3, 4]. TMD nanotubes have a number of interesting properties including high tensile strength [8, 9, 10, 11], mechanically tunable electronic properties [12, 13, 14, 15, 16, 17, 18], and low cytotoxicity [19]. These properties make TMD nanotubes suited to a number of applications, including reinforcement of composites [20, 21, 22, 23, 24, 25], nanoelectromechanical (NEMS) devices [26, 18, 27], and medicine [28], where knowledge of their mechanical properties is important from the perspective of both design and performance.

In view of the above, there have been a number of efforts to characterize the elastic properties of TMD nanotubes, both experimentally [29, 10, 30, 31] and theoretically [12, 32, 33, 34, 17, 35, 36, 37, 14, 38, 39]. However, these studies are limited to only a few TMDs, and that too only for the case of axial tension/compression. In particular, determining the torsional moduli for these systems — relevant for applications such as resonators in NEMS devices [27, 26, 18] — has been limited to very few experimental [40, 27, 18] and theoretical [41, 42] research works, and that too only for a couple of materials. Indeed, the study of torsional deformations at practically relevant twists and nanotube diameters is intractable to ab initio methods like Kohn-Sham density functional theory (DFT) [43, 44] — expected to provide higher fidelity than tight binding and force field calculations for nanoscale systems — given the large number of atoms that are required when employing the standard periodic boundary conditions [45]. Therefore, accurate estimates for a fundamental mechanical property like torsional modulus is not available for TMD nanotubes, which provides the motivation for the current work.

In this work, we calculate the torsional moduli of forty-five select single-walled armchair and zigzag TMD nanotubes using Kohn-Sham DFT. Specifically, considering nanotubes that have been synthesized or are expected to be so in the future, we perform symmetry-adapted DFT calculations to calculate the torsional moduli of these materials at practically relevant twists and nanotube diameters. We find the following relation for the torsional moduli values: $MS_2 > MSe_2 > MTe_2$. In addition, we find that the moduli display a power law dependence on diameter, with a scaling that is generally close to cubic, as predicted by the isotropic elastic continuum model. In particular, the shear moduli so determined are in good agreement with that predicted by the isotropic relation in terms of the Young's modulus and Poisson's ratio, both of which are also calculated here using symmetry-adapted DFT. We also develop a linear regression model for the torsional moduli of TMD nanotubes based on the nature and characteristics of the metal-chalcogen bond, and show that it is capable of making reasonably accurate predictions.

The remainder of the manuscript is organized as follows. In Section 2, we discuss the chosen TMD nanotubes and describe the symmetry-adapted DFT simulations for calculation of their torsional moduli. Next, we present and discuss the results obtained

in Section 3. Finally, we provide concluding remarks in Section 4.

2. Systems and methods

We consider the following single-walled TMD nanotubes with 2H-t symmetry [46, 47]: M={V, Nb, Ta, Cr, Mo, W, Fe, Cu} and X={S, Se, Te}; and the following ones with 1T-o symmetry [46, 47]: M={Ti, Zr, Hf, Mn, Ni, Pd, Pt} and X={S, Se, Te}. These materials have been selected among all the possible transition metal-chalcogen combinations as they have either been synthesized as single/multi-walled nanotubes [48, 49, 50, 51, 46, 52, 53, 54, 55] or the corresponding two-dimensional atomic monolayers have been predicted to be stable from ab initio calculations [5, 56, 57]. The radii for these nanotubes have been chosen so as to be commensurate with those that have been experimentally synthesized, and in cases where such data is not available, we choose radii commensurate with synthesized nanotubes that are expected to have similar structure.

We utilize the Cyclix-DFT code [45] — adaptation of the state-of-the-art real-space DFT code SPARC [58, 59, 60] to cylindrical and helical coordinate systems, with the ability to exploit cyclic and helical symmetry in one-dimensional nanostructures [45, 61, 62] — to calculate the torsional moduli of the aforementioned TMD nanotubes in the low twist limit. Specifically, we consider three-atom unit cell/fundamental domains that has one metal atom and two chalcogen atoms, as illustrated in Fig. 1. Indeed, such calculations are impractical without the symmetry adaption, e.g., a (57,57) MoS_2 nanotube (diameter ~ 10 nm) with an external twist of 2×10^{-4} rad/Bohr has $234,783$ atoms in the simulation domain when employing periodic boundary conditions, well beyond the reach of even state-of-the-art DFT codes on large-scale parallel machines [63, 64, 58]. It is worth noting that the Cyclix-DFT code has already been successfully employed for the study of physical applications [65, 66, 45, 67], which provides evidence of its accuracy.

We employ optimized norm-conserving Vanderbilt (ONCV) [68] pseudopotentials from the SG15 [69] collection and the semilocal Perdew–Burke–Ernzerhof (PBE) [70] exchange-correlation functional. Apart from the tests by the developers [69], we have verified the transferability of the chosen pseudopotentials by comparisons with all-electron DFT code Elk [71] for select bulk systems. In addition, we have found that the equilibrium geometries of the nanotubes and their two-dimensional counterparts (Supplementary Material) are in very good agreement with previous DFT results [5, 6, 32, 36, 14, 72, 73, 74, 57]. There is also very good agreement with experimental measurements [50, 75, 46, 48], confirming the suitability of the chosen exchange-correlation functional. Since we are interested in torsional moduli for the low-twist regime — corresponds to small (linear) perturbations of electron density from the undeformed nanotube — the use of more sophisticated functionals and/or inclusion of relativistic effects through spin orbit coupling (SOC) are not expected to change the results noticeably, especially considering that significant error cancellations occur while

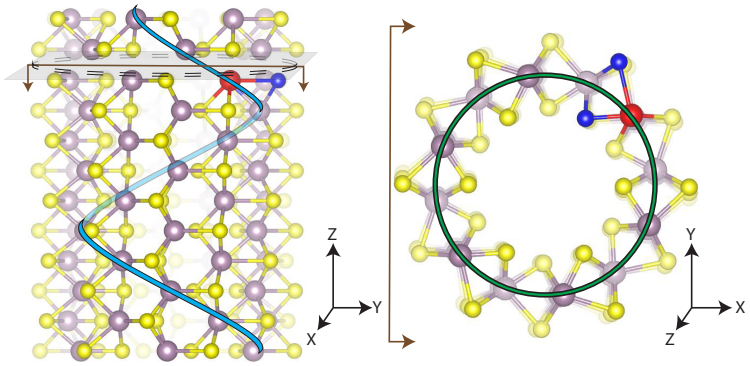

Figure 1: Illustration showing the cyclic and helical symmetry present in a twisted (6,6) TMD nanotube with 2H-t symmetry. In particular, all atoms in the nanotube can be considered to be cyclic and/or helical images of the metal and chalcogen atoms that have been colored red and blue, respectively. This symmetry is exploited while performing electronic structure simulations using the Cyclix-DFT code [45].

taking differences in energy. This is evidenced by the small differences in the ground state electron density between PBE and more sophisticated hybrid functionals for the TMD monolayer systems, even in the presence of SOC [67].

We calculate the torsional modulus in the low-twist regime by first performing ground state DFT simulations for various twisted configurations of the nanotube, and then fitting the data to the following quadratic relation:

$$\mathcal{E}(d,\theta) = \mathcal{E}(d,0) + \frac{1}{2}K(d)\theta^2\,, \tag{1}$$

where K is the torsional modulus, d is the diameter of the nanotube, and θ and $\mathcal{E}$ are the twist and ground state energy densities, respectively, i.e., defined per unit length of the nanotube. Indeed, small enough twists are chosen so that linear response is observed, i.e., the torsional modulus is independent of the twist (Supplementary Material). It is important to note that the resulting shear strains — quantity that better describes the behavior/response of nanotubes, by allowing systematic comparison between tubes with different diameters — are commensurate with those found in torsion experiments [18, 27, 40]. All numerical parameters in Cyclix-DFT, including grid spacing, number of points for Brillouin zone integration, vacuum in the radial direction, and structural relaxation tolerances (both cell and atom) are chosen such that the computed torsional moduli are numerically accurate to within 1% of their reported value. In terms of the energy, this translates to the value at the structural and electronic ground state being converged to within 10^{-5} Ha/atom, a relatively stringent criterion that is necessary to capture the extremely small energy differences that occur at low values of twist.

3. Results and discussion

As described in the previous section, we utilize symmetry-adapted DFT simulations to calculate torsional moduli of the forty-five select armchair and zigzag TMD nanotubes.

The simulation data for all the results presented here can be found in the Supplementary Material. Observing a power law dependence of the torsional modulus with nanotube diameter d, we fit the data to the following relation:

$$K(d) = kd^{\alpha} + K(0)\,, \tag{2}$$

where k and α will be henceforth referred to as the torsional modulus coefficient and exponent, respectively. The values so obtained for the different materials are presented in Table 1. Observing that the exponents are generally close to $\alpha = 3$, in order to enable comparison between the different materials that can have nanotubes with significantly different diameters, we also fit the data to the relation:

$$K(d) = \hat{k}d^{3} + K(0)\,, \tag{3}$$

where $\hat{k}$ is referred to as the average torsional modulus coefficient. The results so obtained are presented through violin plots in Figure 2.

Table 1: Torsional modulus coefficient (k) and exponent (α) for the forty-five select armchair and zigzag TMD nanotubes.

M	Diameter range (nm)	MS_2		MSe_2		MTe_2	
		Torsional modulus coefficient k (eV nm$^{1-\alpha}$) and exponent α		Torsional modulus coefficient k (eV nm$^{1-\alpha}$) and exponent α		Torsional modulus coefficient k (eV nm$^{1-\alpha}$) and exponent α	
		Armchair	Zigzag	Armchair	Zigzag	Armchair	Zigzag
W	2 - 10	267 (3.02)	256 (3.04)	226 (3.03)	230 (3.01)	179 (3.04)	158 (3.09)
Mo	2 - 10	232 (3.03)	213 (3.07)	197 (3.03)	175 (3.09)	150 (3.03)	143 (3.04)
Cr	6 - 10	194 (3.08)	222 (2.98)	171 (3.00)	178 (2.99)	135 (2.95)	191 (2.76)
V	6 - 10	161 (3.07)	170 (3.00)	149 (3.00)	133 (3.00)	98 (2.98)	92 (2.97)
Ta	14 - 40	158 (3.07)	205 (2.95)	176 (2.97)	160 (2.97)	165 (2.85)	155 (2.86)
Nb	2 - 14	133 (3.08)	181 (2.92)	140 (3.00)	162 (2.91)	90 (3.01)	66 (3.17)
Pt	6 - 10	154 (3.01)	156 (3.00)	127 (3.01)	129 (3.00)	133 (2.92)	259 (2.53)
Hf	6 - 30	162 (3.00)	165 (2.98)	136 (3.00)	135 (2.99)	93 (3.00)	85 (3.02)
Zr	6 - 30	149 (3.00)	160 (2.96)	125 (3.00)	127 (2.98)	98 (2.93)	84 (2.98)
Ti	2 - 10	140 (3.03)	153 (2.98)	106 (3.08)	127 (2.94)	75 (3.03)	83 (2.93)
Ni	6 - 10	147 (2.99)	147 (3.00)	127 (2.93)	120 (2.98)	136 (2.63)	156 (2.53)
Pd	6 - 10	114 (3.02)	119 (2.99)	94 (3.02)	100 (2.98)	107 (2.85)	223 (2.40)
Mn	6 - 10	108 (3.08)	122 (3.00)	39 (3.23)	29 (3.38)	27 (3.40)	52 (2.99)
Fe	6 - 10	60 (3.26)	49 (3.29)	102 (2.90)	157 (2.71)	76 (2.87)	109 (2.66)
Cu	6 - 10	30 (3.19)	32 (3.13)	27 (3.14)	49 (2.76)	35 (3.20)	102 (2.35)

We observe that the torsional modulus coefficients span around an order of magnitude between the different materials, with WS_2 and $CuSe_2$ having the largest and smallest values, respectively. Notably, even the largest value obtained here is nearly three times smaller than the carbon nanotube (733 eV/nm^2) [45], which can be

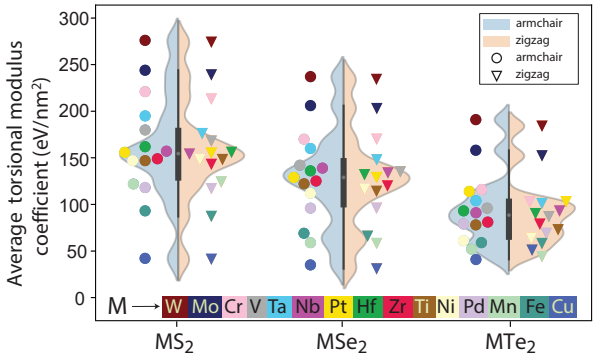

Figure 2: Average torsional modulus coefficient ($\hat{k}$) for the forty-five select armchair and zigzag TMD nanotubes.

attributed to the extremely strong covalent carbon-carbon bonds. In comparison with experiments, where only the torsional modulus of WS_2 has been measured to date (∼384 eV/nm^2) [18], there is good agreement with the average torsional modulus coefficient reported here (275 eV/nm^2). In particular, the computed value is well within the error bound communicated for the experimental result. In comparison with theoretical predictions, where only the values for MoS_2 are available from force field (armchair: 249 eV/nm^2 and zigzag: 243 eV/nm^2) [42] and tight binding (armchair: 265 eV/nm^2 and zigzag: 265 eV/nm^2) [41] simulations, there is good agreement with the average torsional modulus coefficients reported here (armchair: 244 eV/nm^2 and zigzag: 239 eV/nm^2). Overall, we observe that the torsional moduli values generally follow the trend $MS_2 > MSe_2 > MTe_2$. This can be explained by the metal-chalcogen bond length having the reverse trend, with shorter bonds generally expected to be stronger due to the increase in orbital overlap.

We also observe from the results in Table 1 that the torsional modulus exponents are in the neighborhood of $\alpha = 3$, in agreement with the isotropic elastic continuum model [76]. In such an idealization, the shear modulus G can be calculated from the torsional modulus coefficient using the following relation derived from the continuum analysis of a homogeneous isotropic circular tube subject to torsional deformations‡:

$$G = \frac{\hat{k}}{2\pi}\,. \tag{4}$$

The results so obtained are presented in Figure 3. Note that since there are some noticeable deviations from $\alpha = 3$ (Table 1) — suggests that the shear modulus changes with diameter — the results in Figure 3 correspond to the case when $\hat{k}$ is determined from the single data point corresponding to the largest diameter nanotube studied for

‡ Since there is only a single parameter (i.e., shear modulus) in the continuum model, it can be determined from the average torsional modulus coefficient using Equation 4. In the case of discrete finite-element models of nanotubes [77, 78], which can provide significant computational efficiency relative to ab initio methods for studying mechanical behavior, a number of other DFT simulations would need to be performed to determine the force constants inherent to such models.

each material. To verify their isotropic nature, we also determine the shear moduli of the nanotubes as predicted by the isotropic relation in terms of the Young's modulus (E) and Poisson's ratio (ν): $G = E/2(1+\nu)$, both of which are also calculated using Cyclix-DFT, the results of which are summarized in Figure 3. It is clear that there is very good agreement between the computed and predicted shear moduli, suggesting that TMD nanotubes can be considered to be elastically isotropic.

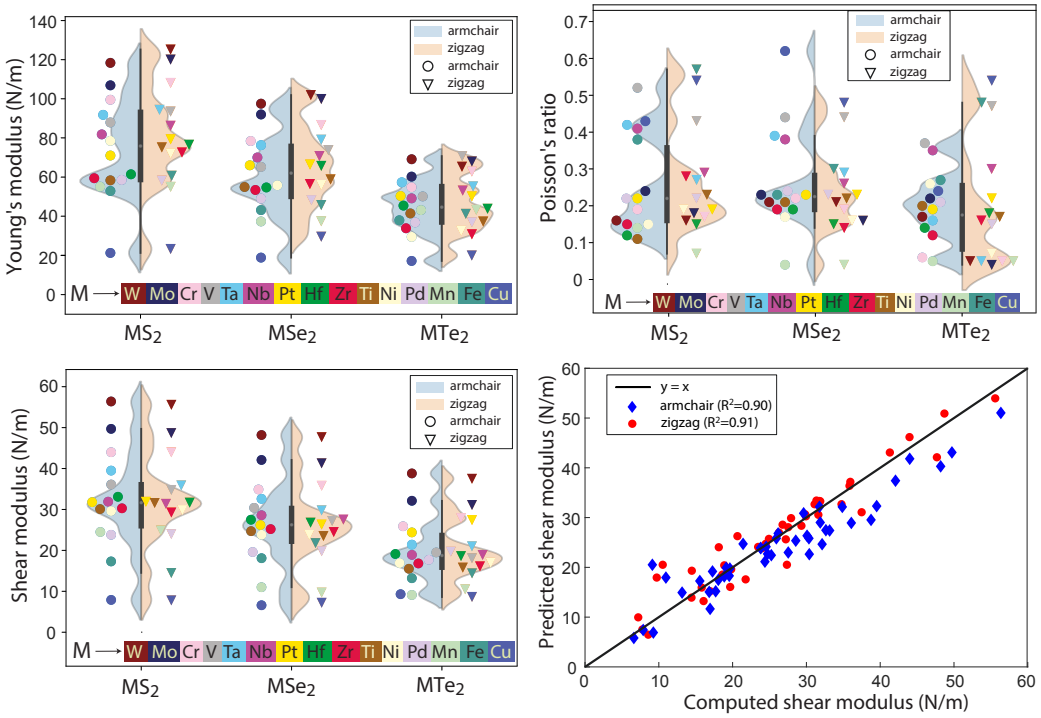

Figure 3: Young's modulus (E), shear modulus (G), and Poisson's ratio (ν) of the forty-five select armchair and zigzag TMD nanotubes. The predicted shear modulus refers to that obtained from the isotropic relation in terms of the Young's modulus and Poisson's ratio. The values of R^2 shown in the legend denotes the coefficient of determination for the linear regression. The results correspond to the largest diameter nanotube that has been studied for each material.

We observe from the results in Figure 3 that the Young's moduli follow a similar trend as the torsional modulus coefficients and therefore the shear moduli, which can be again explained by the strength of the metal-chalcogen bond, consistent with results obtained for molybdenum and tungsten TMD monolayers [79, 80, 81]. In regards to the Poisson's ratio, we find that the MnS_2, $MnSe_2$, $MnTe_2$, $CrTe_2$, WTe_2, $MoTe_2$, $TaTe_2$, and $NiTe_2$ nantotubes have a value near zero. In addition, the CuS_2, $CuSe_2$, $CuTe_2$, VS_2 and FeS_2 nanotubes have ν greater than the isotropic theoretical limit of 0.5, which can be justified by the anistropic nature of these materials — evidenced by the relatively poor agreement between the predicted and computed shear moduli (Figure 3) — where this bound is not applicable [82]. In regards to failure of these materials, it is possible to use Frantsevich's rule [83] — materials with $\nu > 0.33$ and $\nu < 0.33$ are expected

to be ductile and brittle, respectively — to predict that M={Cu, Nb, Fe, Ta and V} nanotubes are ductile and M={W, Mo, Cr, Pt, Hf, Zr, Ti, Ni, Pd, Mn} are brittle. In particular, there is a clear divide between the Poisson's ratio of these two sets, as seen in Figure 3. Note that the computed Young's moduli and Poisson's ratio values are in good agreement with those available in literature [12, 41, 32, 33, 17, 37], further confirming the fidelity of the simulations performed here.

The above results indicate that the torsional moduli of TMD nanotubes are dependent on the nature and strength of the metal-chalcogen bond, which can be expected to depend on the bond length, difference in electronegativity between the atoms, and sum of their ionization potential and electron affinity. The first feature mentioned above is used to mainly capture the strength of the bond, and the other two features are used to mainly capture the nature of the bonding [84, 85, 86, 87]. Using these three features, we perform a linear regression on the set of average torsional modulus coefficients, the results of which are presented in Figure 4. The fit is reasonably good, suggesting that the features chosen here play a significant role in determining the torsional moduli of TMD nanotubes. Note that inclusion of the bond angle as a feature did not improve the quality of the fit, and therefore has been neglected here. Also note that though the quality of the fit can be further increased by using higher order polynomial regression, it can possibly lead to overfitting, and is hence not adopted here.

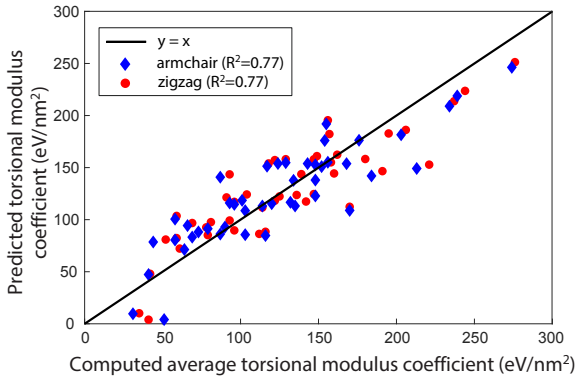

Figure 4: The set of computed average torsional modulus coefficients ($\hat{k}$) and its linear regression with the features being the metal-chalcogen bond length, difference in electronegativity between the metal and chalcogen atoms, and sum of the metal's ionization potential and chalcogen's electron affinity. The values of R^2 shown in the legend denotes the coefficient of determination for the linear regression.

4. Concluding remarks

We have calculated the torsional moduli of forty-five select single-walled TMD nanotubes using *ab initio* DFT simulations. Specifically, we have computed torsional moduli for the armchair and zigzag variants of the chosen TMD nanotubes at practically relevant twists and nanotube diameters, while considering materials that have been synthesized

or are likely to be synthesized. We have found that the variation of the torsional moduli values between the different nanotubes follows the trend: $MS_2 > MSe_2 > MTe_2$. In addition, we have found that the moduli display a power law dependence on the diameter, with the scaling generally close to cubic, as predicted by the isotropic elastic continuum model. In particular, the shear moduli so determined have been found to be in good agreement with that predicted by the isotropic relation in terms of the Young's modulus and Poisson's ratio, both of which have also been calculated in this work from DFT simulations. Finally, we have developed a linear regression model for the torsional moduli of TMD nanotubes that is based on the nature and characteristics of the metal-chalcogen bond, and have shown that it is capable of making reasonably accurate predictions.

In regards to future research, given their significant applications in semiconductor devices, the electromechanical response of TMD nanotubes to torsional deformations presents itself as an interesting topic worthy of pursuit. In addition, given the plethora of multi-walled TMD nanotubes that have been synthesized, studying their mechanical and electronic response to torsional deformations also presents itself as a worthy subject of investigation.

Acknowledgments

The authors gratefully acknowledge the support of the U.S. National Science Foundation (CAREER-1553212 and MRI-1828187). P.S. acknowledges discussions with Arash Yavari regarding anisotropic elasticity.

Conflicts of interest

There are no conflicts to declare.

References

[1] S Iijima. Helical microtubules of graphitic carbon. *Nature*, 354(6348):56–58, 1991.

[2] R Tenne. Advances in the synthesis of inorganic nanotubes and fullerene-like nanoparticles. *Angewandte Chemie International Edition*, 42(42):5124–5132, 2003.

[3] C N R Rao and M Nath. Inorganic nanotubes. In *Advances In Chemistry: A Selection of CNR Rao's Publications (1994–2003)*, pages 310–333. World Scientific, 2003.

[4] M Serra, R Arenal, and R Tenne. An overview of the recent advances in inorganic nanotubes. *Nanoscale*, 11(17):8073–8090, 2019.

[5] S Haastrup, M Strange, M Pandey, T Deilmann, P S Schmidt, N F Hinsche, M N Gjerding, D Torelli, P M Larsen, A C Riis-Jensen, et al. The Computational 2D Materials Database: high-throughput modeling and discovery of atomically thin crystals. *2D Materials*, 5(4):042002, 2018.

[6] J Zhou, L Shen, M D Costa, K A Persson, Shyue P Ong, P Huck, Y Lu, X Ma, Y Chen, H Tang, et al. 2DMatPedia, an open computational database of two-dimensional materials from top-down and bottom-up approaches. *Scientific Data*, 6(1):1–10, 2019.

[7] M N Gjerding, A Taghizadeh, A Rasmussen, S Ali, F Bertoldo, T Deilmann, U P Holguin, N R Knøsgaard, M Kruse, S Manti, et al. Recent Progress of the Computational 2D Materials Database (C2DB). *arXiv preprint arXiv:2102.03029*, 2021.

[8] A Kis, D Mihailovic, M Remskar, A Mrzel, A Jesih, I Piwonski, A J Kulik, W Benoît, and L Forró. Shear and Young's moduli of MoS_2 nanotube ropes. *Advanced Materials*, 15(9):733–736, 2003.

[9] I Kaplan-Ashiri and R Tenne. Mechanical properties of WS_2 nanotubes. *Journal of Cluster Science*, 18(3):549–563, 2007.

[10] I Kaplan-Ashiri, S R Cohen, K Gartsman, V Ivanovskaya, T Heine, G Seifert, I Wiesel, H D Wagner, and R Tenne. On the mechanical behavior of WS_2 nanotubes under axial tension and compression. *Proceedings of the National Academy of Sciences*, 103(3):523–528, 2006.

[11] D-M Tang, X Wei, M-S Wang, N Kawamoto, Y Bando, C Zhi, M Mitome, A Zak, R Tenne, and D Golberg. Revealing the anomalous tensile properties of WS_2 nanotubes by in situ transmission electron microscopy. *Nano Letters*, 13(3):1034–1040, 2013.

[12] N Zibouche, M Ghorbani-Asl, T Heine, and A Kuc. Electromechanical properties of small transition-metal dichalcogenide nanotubes. *Inorganics*, 2(2):155–167, 2014.

[13] S Oshima, M Toyoda, and S Saito. Geometrical and electronic properties of unstrained and strained transition metal dichalcogenide nanotubes. *Physical Review Materials*, 4(2):026004, 2020.

[14] W Li, G Zhang, M Guo, and Y-W Zhang. Strain-tunable electronic and transport properties of MoS_2 nanotubes. *Nano Research*, 7(4):518–527, 2014.

[15] M Ghorbani-Asl, N Zibouche, M Wahiduzzaman, A F Oliveira, A Kuc, and T Heine. Electromechanics in MoS_2 and WS_2: nanotubes vs. monolayers. *Scientific Reports*, 3:2961, 2013.

[16] P Lu, X Wu, W Guo, and X C Zeng. Strain-dependent electronic and magnetic properties of MoS_2 monolayer, bilayer, nanoribbons and nanotubes. *Physical Chemistry Chemical Physics*, 14(37):13035–13040, 2012.

[17] R Ansari, S Malakpour, M Faghihnasiri, and S Sahmani. An ab initio investigation into the elastic, structural and electronic properties of MoS_2 nanotubes. *Superlattices and Microstructures*, 82:188–200, 2015.

[18] R Levi, J Garel, D Teich, G Seifert, R Tenne, and E Joselevich. Nanotube electromechanics beyond carbon: the case of WS_2. *ACS Nano*, 9(12):12224–12232, 2015.

[19] M Pardo, T Shuster-Meiseles, S Levin-Zaidman, A Rudich, and Y Rudich. Low cytotoxicity of inorganic nanotubes and fullerene-like nanostructures in human bronchial epithelial cells: relation to inflammatory gene induction and antioxidant response. *Environmental Science & Technology*, 48(6):3457–3466, 2014.

[20] M Shtein, R Nadiv, N Lachman, H D Wagner, and O Regev. Fracture behavior of nanotube–polymer composites: Insights on surface roughness and failure mechanism. *Composites Science and Technology*, 87:157–163, 2013.

[21] G Otorgust, H Dodiuk, S Kenig, and R Tenne. Important insights into polyurethane nanocomposite-adhesives; a comparative study between INT-WS_2 and CNT. *European Polymer Journal*, 89:281–300, 2017.

[22] D M Simić, D B Stojanović, M Dimić, K Mišković, M Marjanović, Z Burzić, P S Uskoković, A Zak, and R Tenne. Impact resistant hybrid composites reinforced with inorganic nanoparticles and nanotubes of WS_2. *Composites Part B: Engineering*, 176:107222, 2019.

[23] R Nadiv, M Shtein, M Refaeli, A Peled, and O Regev. The critical role of nanotube shape in cement composites. *Cement and Concrete Composites*, 71:166–174, 2016.

[24] S-J Huang, C-H Ho, Y Feldman, and R Tenne. Advanced AZ31 Mg alloy composites reinforced by WS_2 nanotubes. *Journal of Alloys and Compounds*, 654:15–22, 2016.

[25] M Naffakh, A M Diez-Pascual, and C Marco. Polymer blend nanocomposites based on poly (l-lactic acid), polypropylene and WS_2 inorganic nanotubes. *RSC Advances*, 6(46):40033–40044, 2016.

[26] D Yudilevich, R Levi, I Nevo, R Tenne, A Ya'akobovitz, and E Joselevich. Self-sensing torsional resonators based on inorganic nanotubes. *ICME*, 2018.

[27] Y Divon, R Levi, J Garel, D Golberg, R Tenne, A Ya'akobovitz, and E Joselevich. Torsional resonators based on inorganic nanotubes. *Nano Letters*, 17(1):28–35, 2017.

[28] G Lalwani, A M Henslee, B Farshid, P Parmar, L Lin, Y-X Qin, F K Kasper, A G Mikos, and B Sitharaman. Tungsten disulfide nanotubes reinforced biodegradable polymers for bone tissue engineering. *Acta Biomaterialia*, 9(9):8365–8373, 2013.

[29] I Kaplan-Ashiri, S R Cohen, K Gartsman, R Rosentsveig, G Seifert, and R Tenne. Mechanical behavior of individual WS_2 nanotubes. *Journal of Materials Research*, 19(2):454–459, 2004.

[30] M S Wang, I Kaplan-Ashiri, X L Wei, R Rosentsveig, H D Wagner, R Tenne, and L M Peng. In situ TEM measurements of the mechanical properties and behavior of WS_2 nanotubes. *Nano Research*, 1(1):22, 2008.

[31] A Grillo, M Passacantando, A Zak, A Pelella, and A D Bartolomeo. WS_2 Nanotubes: Electrical conduction and field emission under electron irradiation and mechanical stress. *Small*, 16(35):2002880, 2020.

[32] Y Z Wang, R Huang, X Q Wang, Q F Zhang, B L Gao, L Zhou, and G Hua. Strain-tunable electronic properties of CrS_2 nanotubes. *Chalcogenide Letters*, 13(7):301–307, 2016.

[33] A V Bandura, S I Lukyanov, R A Evarestov, and D D Kuruch. Calculation of Young's modulus of MoS_2-based single-wall nanotubes using force-field and hybrid density functional theory. *Physics of the Solid State*, 60(12):2551–2558, 2018.

[34] Q-L Xiong, J Zhang, C Xiao, and Z-H Li. Effects of atomic vacancies and temperature on the tensile properties of single-walled MoS_2 nanotubes. *Physical Chemistry Chemical Physics*, 19(30):19948–19958, 2017.

[35] P Ying, J Zhang, J Zhou, Q Liang, and Z Zhong. Mechanical behaviors of MoS nanowires under tension from molecular dynamics simulations. *Computational Materials Science*, 179:109691, 2020.

[36] J Xiao, M Long, X Li, H Xu, H Huang, and Y Gao. Theoretical prediction of electronic structure and carrier mobility in single-walled MoS_2 nanotubes. *Scientific Reports*, 4(1):1–7, 2014.

[37] T Lorenz, D Teich, J-O Joswig, and G Seifert. Theoretical study of the mechanical behavior of individual TiS_2 and MoS_2 nanotubes. *The Journal of Physical Chemistry C*, 116(21):11714–11721, 2012.

[38] V Sorkin, H Pan, H Shi, S Y Quek, and Y W Zhang. Nanoscale transition metal dichalcogenides: structures, properties, and applications. *Critical Reviews in Solid State and Materials Sciences*, 39(5):319–367, 2014.

[39] E Kalfon-Cohen, D Barlam, O Tevet, and S R Cohen. Insights on uniaxial compression of WS_2 inorganic fullerenes: A finite element study. *Journal of Materials Research*, 27(1):161, 2012.

[40] K S Nagapriya, O Goldbart, I Kaplan-Ashiri, G Seifert, R Tenne, and E Joselevich. Torsional stick-slip behavior in WS_2 nanotubes. *Physical Review Letters*, 101(19):195501, 2008.

[41] D-B Zhang, T Dumitrică, and G Seifert. Helical nanotube structures of MoS_2 with intrinsic twisting: an objective molecular dynamics study. *Physical Review Letters*, 104(6):065502, 2010.

[42] E W Bucholz and S B Sinnott. Mechanical behavior of MoS_2 nanotubes under compression, tension, and torsion from molecular dynamics simulations. *Journal of Applied Physics*, 112(12):123510, 2012.

[43] P Hohenberg and W Kohn. Inhomogeneous electron gas. *Physical Review*, 136(3B):B864, 1964.

[44] W Kohn and L J Sham. Self-consistent equations including exchange and correlation effects. *Physical Review*, 140(4A):A1133, 1965.

[45] A Sharma and P Suryanarayana. Real-space density functional theory adapted to cyclic and helical symmetry: Application to torsional deformation of carbon nanotubes. *Physical Review B*, 103(3):035101, 2021.

[46] M Nath and C N R Rao. Nanotubes of group 4 metal disulfides. *Angewandte Chemie International Edition*, 41(18):3451–3454, 2002.

[47] A V Bandura and R A Evarestov. TiS_2 and ZrS_2 single-and double-wall nanotubes: First-principles study. *Journal of Computational Chemistry*, 35(5):395–405, 2014.

[48] M Nath and C N R Rao. $MoSe_2$ and WSe_2 nanotubes and related structures. *Chemical Communications*, 1(21):2236–2237, 2001.

[49] M Nath, A Govindaraj, and C N R Rao. Simple synthesis of MoS_2 and WS_2 nanotubes. *Advanced Materials*, 13(4):283–286, 2001.

[50] J Chen, S-L Li, Z-L Tao, Y-T Shen, and C-X Cui. Titanium disulfide nanotubes as hydrogen-storage materials. *Journal of the American Chemical Society*, 125(18):5284–5285, 2003.

[51] M Nath and C N R Rao. New metal disulfide nanotubes. *Journal of the American Chemical Society*, 123(20):4841–4842, 2001.

[52] A R Tenne, L Margulis, M Genut, and G Hodes. Polyhedral and cylindrical structures of tungsten disulphide. *Nature*, 360(6403):444–446, 1992.

[53] J M Gordon, E A Katz, D Feuermann, Ana Albu-Yaron, M Levy, and R Tenne. Singular MoS_2, SiO_2 and Si nanostructures—synthesis by solar ablation. *Journal of Materials Chemistry*, 18(4):458–462, 2008.

[54] V Brüser, R Popovitz-Biro, A Albu-Yaron, T Lorenz, G Seifert, R Tenne, and A Zak. Single-to triple-wall WS_2 nanotubes obtained by high-power plasma ablation of WS_2 multiwall nanotubes. *Inorganics*, 2(2):177–190, 2014.

[55] M Remskar, A Mrzel, Z Skraba, A Jesih, M Ceh, J Demšar, P Stadelmann, F Lévy, and D Mihailovic. Self-assembly of subnanometer-diameter single-wall MoS_2 nanotubes. *Science*, 292(5516):479–481, 2001.

[56] T Heine. Transition metal chalcogenides: ultrathin inorganic materials with tunable electronic properties. *Accounts of Chemical Research*, 48(1):65–72, 2015.

[57] H Guo, N Lu, L Wang, X Wu, and X C Zeng. Tuning electronic and magnetic properties of early transition-metal dichalcogenides via tensile strain. *The Journal of Physical Chemistry C*, 118(13):7242–7249, 2014.

[58] Q Xu, A Sharma, B Comer, H Huang, E Chow, A J Medford, J E Pask, and P Suryanarayana. SPARC: Simulation Package for Ab-initio Real-space Calculations. *arXiv preprint arXiv:2005.10431*, 2020.

[59] S Ghosh and P Suryanarayana. SPARC: Accurate and efficient finite-difference formulation and parallel implementation of density functional theory: Isolated clusters. *Computer Physics Communications*, 212:189–204, 2017.

[60] S Ghosh and P Suryanarayana. SPARC: Accurate and efficient finite-difference formulation and parallel implementation of Density Functional Theory: Extended systems. *Computer Physics Communications*, 216:109–125, 2017.

[61] S Ghosh, A S Banerjee, and P Suryanarayana. Symmetry-adapted real-space density functional theory for cylindrical geometries: Application to large group-IV nanotubes. *Physical Review B*, 100(12):125143, 2019.

[62] A S Banerjee and P Suryanarayana. Cyclic density functional theory: A route to the first principles simulation of bending in nanostructures. *Journal of the Mechanics and Physics of Solids*, 96:605–631, 2016.

[63] A S Banerjee, L Lin, P Suryanarayana, C Yang, and J E Pask. Two-level Chebyshev filter based complementary subspace method: pushing the envelope of large-scale electronic structure calculations. *Journal of Chemical Theory and Computation*, 14(6):2930–2946, 2018.

[64] P Motamarri, S Das, S Rudraraju, K Ghosh, D Davydov, and V Gavini. DFT-FE–A massively parallel adaptive finite-element code for large-scale density functional theory calculations. *Computer Physics Communications*, 246:106853, 2020.

[65] D Codony, I Arias, and P Suryanarayana. Transversal flexoelectric coefficient for nanostructures at finite deformations from first principles. *Physical Review Materials*, 5(6):L030801, 2021.

[66] S Kumar, D Codony, I Arias, and P Suryanarayana. Flexoelectricity in atomic monolayers from first principles. *Nanoscale*, 13(3):1600–1607, 2021.

[67] S Kumar and P Suryanarayana. Bending moduli for forty-four select atomic monolayers from first principles. *Nanotechnology*, 31(43):43LT01, 2020.

[68] D R Hamann. Optimized norm-conserving Vanderbilt pseudopotentials. *Physical Review B*, 88(8):085117, 2013.

[69] M Schlipf and F Gygi. Optimization algorithm for the generation of ONCV pseudopotentials. *Computer Physics Communications*, 196:36–44, 2015.

[70] J P Perdew, K Burke, and M Ernzerhof. Generalized gradient approximation made simple. *Physical Review Letters*, 77(18):3865, 1996.

[71] The Elk Code. http://elk.sourceforge.net/.

[72] C Ataca, H Sahin, and S Ciraci. Stable, single-layer MX2 transition-metal oxides and dichalcogenides in a honeycomb-like structure. *The Journal of Physical Chemistry C*, 116(16):8983–8999, 2012.

[73] C-H Chang, X Fan, S-H Lin, and J-L Kuo. Orbital analysis of electronic structure and phonon dispersion in MoS_2, $MoSe_2$, WS_2, and WSe_2 monolayers under strain. *Physical Review B*, 88(19):195420, 2013.

[74] B Amin, T P Kaloni, and U Schwingenschlögl. Strain engineering of WS_2, WSe_2, and WTe_2. *RSC Advances*, 4(65):34561–34565, 2014.

[75] M Nath, S Kar, A K Raychaudhuri, and C N R Rao. Superconducting $NbSe_2$ nanostructures. *Chemical Physics Letters*, 368(5-6):690–695, 2003.

[76] A C Ugural and S K Fenster. *Advanced strength and applied elasticity*. Pearson education, 2003.

[77] C Li and T-W Chou. A structural mechanics approach for the analysis of carbon nanotubes. *International Journal of Solids and Structures*, 40(10):2487–2499, 2003.

[78] K I Tserpes and P Papanikos. Finite element modeling of single-walled carbon nanotubes. *Composites Part B: Engineering*, 36(5):468–477, 2005.

[79] R Zhang and R Cheung. *Mechanical Properties and Applications of Two-Dimensional Materials*, chapter 10, pages 219–246. IntechOpen, 2016.

[80] Z Fan, Z Wei-Bing, and T Bi-Yu. Electronic structures and elastic properties of monolayer and bilayer transition metal dichalcogenides MX_2 (M= Mo, W; X= O, S, Se, Te): a comparative first-principles study. *Chinese Physics B*, 24(9):097103, 2015.

[81] N A Pike, A Dewandre, B Van Troeye, X Gonze, and M J Verstraete. Vibrational and dielectric properties of monolayer transition metal dichalcogenides. *Physical Review Materials*, 3(7):074009, 2019.

[82] T C T Ting and T Chen. Poisson's ratio for anisotropic elastic materials can have no bounds. *The Quarterly Journal of Mechanics and Applied Mathematics*, 58(1):73–82, 2005.

[83] I N Frantsevich, F F Voronov, and S A Bokuta. Elastic Moduli of Metals and Insulators Handbook (Kiev), 1983.

[84] N Glebko, I Aleksandrova, G C Tewari, T S Tripathi, M Karppinen, and A J Karttunen. Electronic and vibrational properties of TiS_2, ZrS_2, and HfS_2: Periodic trends studied by dispersion-corrected hybrid density functional methods. *The Journal of Physical Chemistry C*, 122(47):26835–26844, 2018.

[85] R T Sanderson. Electronegativity and bonding of transitional elements. *Inorganic Chemistry*, 25(19):3518–3522, 1986.

[86] M Winter. WebElements [http://www. webelements. com/], University of Sheffield. *UK.(Reference Date: 01/02/2000)*, 2000.

[87] D F C Morris and L H Ahrens. Ionization potentials and the chemical binding and structure of simple inorganic crystalline compounds—I: Chemical binding. *Journal of Inorganic and Nuclear Chemistry*, 3(5):263–269, 1956.